Scientific African 16 (2022) e01266

Contents lists available at ScienceDirect

Scientific African

journal homepage: www.elsevier.com/locate/sciaf

A numerical modelling approach for the optimisation of photovoltaic installations in the mitigation of thermal effects

K. Chiteka[a,*], L. Madiye[b], H. Chingosho[b], R. Arora[c], C.C. Enweremadu[d]

[a] Faculty of Engineering and the Environment, Gwanda State University, P.O Box 30 Filabusi, Zimbabwe
[b] Department of Mechanical Engineering, University of Zimbabwe, Harare, Zimbabwe
[c] Department of Mechanical Engineering, Amity University Haryana, Gurgaon 122413, India
[d] Department of Mechanical and Industrial Engineering, University of South Africa, Florida, South Africa

ARTICLE INFO

Article history:
Received 24 July 2021
Revised 6 April 2022
Accepted 22 June 2022

Editor: DR B Gyampoh

Keywords:
Solar photovoltaics
Thermal effects
Thermal mitigation
Modelling and simulation
Optimisation

ABSTRACT

Solar energy presents one of the best alternative sources of energy in the current bid to mitigate the negative impacts of global warming. The present study evaluated the influence of the installation configuration together with the meteorological parameters on the temperature characteristics of a solar photovoltaic array. Three dimensional simulation using Computational Fluid Dynamics was used in the numerical analysis of the temperature characteristics on solar PV arrays. The Shear Stress Transport k-ω model was employed to analyse the turbulent characteristics of the airstream near the photovoltaic array. A temperature prediction model was developed using Artificial Neural Networks and the model was found to be accurate with a coefficient of determination, R^2 of 93.1 %. A Response Surface Methodology optimization model was developed to maximize energy generation while minimizing solar photovoltaic cell operating temperature. The models were able to reduce temperature and improve energy generated by a 3.9 %. The optimized tilt and azimuth angles were found to be 28.2° tilt and 13.2°, respectively, yielding an average cell temperature of 29.3 °C which gave a 3.9 % increase in energy and revenue generated.

Introduction

Renewable energy sources have gained much attention in the last decade and can provide most of the world's energy needs. The issues to face with global warming and environmental degradation have necessitated the adoption of renewable energy sources, particularly solar energy, which is freely available in abundance [7,14]. As a result many countries have shifted their focus to clean and renewable energy sources [8]. However, solar energy has its own shortcomings which include intermittency and its dependency on meteorological and environmental factors. There are three main factors affecting the performance of solar photovoltaics (PV) and these include irradiance, temperature and soiling [17].

The current PV technology is dominated by crystalline silicone modules contributing 90 % to the global PV market [16]. However, these are greatly affected by temperatures above 25 °C [1,29]. Although heat gain is desirable in solar thermal

* Corresponding author.
E-mail address: kudzanayi.chiteka@gsu.ac.zw (K. Chiteka).

https://doi.org/10.1016/j.sciaf.2022.e01266

List of abbreviations

ABL	Atmospheric Boundary Layer
ANNs	Artificial Neural Networks
ANOVA	analysis of variance
BIPV	building integrated photovoltaics
CCD	central composite design
CFD	computational fluid dynamics
CRF	capital recovery factor
DI	diffuse irradiance
DNI	direct normal irradiance
FVM	finite volume method
GHI	global horizontal irradiance
IR	infrared radiation
IRR	internal rate of return
kWh	kilo-watt-hour
MAPE	mean absolute percentage error
MWh	mega-watt-hour
NASA	national aeronautics and space administration
NNE	north of north east
NNW	north of north west
NPV	net present value
PB	pay back
PSO	particle swarm optimisation
PV	photovoltaic(s)
PWAF	present worth annuity factor
$PWAF_{es}$	present worth annuity factor (Escalated)
RANS	Reynolds Averaged Navier Stokes
RF	random forests
RMSE	residual mean square error
RSM	response surface methodology
SIMPLE	semi-implicit method for pressure linked equations
SOU	second order upwind
SST k-ω	shear stress transport k-ω
TKE	turbulent kinetic energy
UDFs	user defined functions.
FiT	feed - in - tarriff

systems [6,9], it is definitely undesirable in solar PV systems. As the cell temperature increases, the PV array performance reduces considerably [31]. In essence, there is a linear association between power loss and PV array temperature. Many correlations have been developed in studying the relationships between temperature and PV efficiency. For example, studies have indicated a performance loss between 0.1 % and 0.65 %/K due to temperature [16]. This phenomenon justifies the importance of cooling in solar PV arrays mainly in hot climates [33].

Cooling of solar PV collectors is indispensable for improving the power output in solar PV plants [26]. Some temperature mitigation procedures have been proposed and these include water cooling, use of hybrid systems (PV-Thermal), forced air circulation and natural air circulation [30]. Wind or air flow plays a significant role in lowering the array temperature thus improving the performance of the PV array. Mirzaei and Carmeliet [20] evaluated the simultaneous airflow both underneath and above the PV modules to assess the temperature characteristics on the PV array using infrared thermography. It was noted that there was a non-uniform distribution of surface temperature owing to the lateral eddies developed in the flow. In a different study, the role of cavity airflow on PV array performance was investigated using particle image velocimetry and it was found that the upstream velocity can be 1.26 to 1.35 times slower than the airflow in the cavity [21]. The results also indicated that turbulent mixing in a stepped configuration of PV modules yields better performance compared to a flat configuration. Studies have also shown that, air flow, in the form both of forced convection or natural convection, has a cooling effect on the solar PV module [10], thus wind-driven temperature mitigation is therefore widely accepted [33]. Al-Nimr et al. [2] proposed a hybrid wind/PV system to minimize the temperature rise on the PV cells through the use of a wind turbine. It was shown that through this hybrid system, more energy was generated by both the wind turbine and the PV system.

Incorporating the major parameters influencing PV performance in optimising the installation configuration is of great importance. The effects of irradiance and temperature on PV performance have been widely studied [15]. However, these studies mainly concentrated on analysing the effects of these parameters on PV performance [5]. Many studies have only

highlighted the importance of irradiance on optimisation of the installation configuration. Some studies have proposed the incorporation of other parameters such as soiling and shading in the optimisation of the installation configuration [3,17]. However, the effect of temperature has not been fully investigated. Attempts have been made to evaluate the effects of cooling on PV array performance, and it was reported that increasing wind speeds improves the PV array performance [12].

Under normal circumstances factors which include wind speed and direction have a substantial contribution on the PV cell temperature although its analysis is complex due to the stochastic nature of wind. However, if the cooling effect of wind is taken into consideration, the optimum installation configuration can be different from the generally accepted configuration. The optimisation of installation configuration to utilise the cooling effect of wind is still yet to be investigated. Previous studies were mainly concerned on the cooling effect of wind flow on solar photovoltaics (PV) systems. The optimisation of such systems to maximise power generation while minimising the thermal effects has not been widely considered. The generally accepted optimum PV installation configuration only take the solar irradiance into consideration. The influence of other important factors such as temperature and the possible mitigation approaches for maximum energy yield have been generally overlooked. In the optimisation of the configuration of a PV array installation, there is a need to consider other factors such as temperature effects. Although it is a complex approach, this will lead to a better optimisation model and higher energy yields. If installations are optimised, higher energy yields are obtained and this improves the revenues generated. This study therefore focuses on developing a predictive model for PV array temperature and establish an optimisation model to minimise temperature effects while maximising energy yield. The study is based on the premise that, of the major parameters influencing solar energy yield, i.e. irradiance, temperature and soiling, irradiance has been widely investigated and installation optimisation has been studied based on irradiance. However, temperature is also an important factor which needs to be considered for determining the optimal installation configuration.

This research study is organised as follows; section 1 introduces the issues of thermal effects on PV performance. The related literature is also scanned in light of the present study. Section 2 presents the research approaches and methods used in this study. These include the experimental setup, the simulation approaches and techniques used. The data collection and validation mechanisms used are also discussed in this section. Section 3 outlines and discusses the results obtained from the simulation analysis. The techno-economic and optimisation analysis of the present study is also considered in this section leading to the conclusions in Section 4.

Materials and methods

The study area of Harare in Zimbabwe with latitude 17.8°, longitude of 31.05°E and elevation of 1495m was chosen in this study. This location is characterized by two main seasons which are summer and winter. Summer begins in September and ends in April while winter ranges from May to August. Violent wind speeds are not experienced in this area and the average temperatures range from 19° – 31° depending on the month. Recent measured solar irradiance data is not available for this location due to non-functioning equipment.

The initial step involved feature extraction from a wide array of meteorological parameters which was done to select the best parameters for predictive modelling and simulation. This was followed by the development of a temperature predictive model using selected meteorological parameters. The third step involved simulations on solar energy generated under varying tilt and azimuth (also known as orientation) angles. Having ascertained the implications on energy of varying the tilt and orientation, experimental design was performed to determine the minimum number of simulations that can be run in CFD. The simulations were run and on each simulation the average and maximum cell temperature were recorded and this was used to determine the thermal losses for each simulated configuration. These thermal losses were used as input in PVSyst for energy simulations. This was followed by optimisation for both temperature minimisation and energy maximisation. Finally, to determine the effectiveness of the optimisation model in financial terms, an economic analysis was done. Fig. 1 provides the steps followed in this study from feature selection, temperature predictive modelling, experimental design, CFD thermal simulations, energy simulations, optimisation and economic analysis.

Parameter correlation and dimensionality reduction

Parameter correlation was performed to establish the relationships between the different meteorological parameters with temperature. Fourteen environmental and meteorological parameters were obtained from "NASA Solar Energy and Surface

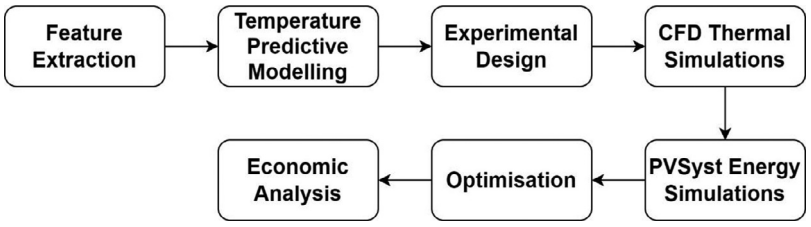

Fig. 1. Visual summary of the methodology followed in the study.

Meteorology" for use in temperature prediction and optimisation modelling. The meteorological parameters used are; precipitation (R), surface pressure (P), relative humidity (H), Diffuse Irradiance (DI), Global Horizontal Irradiance (GHI), Direct Normal Irradiance (DNI), minimum wind speed (W_{min}), maximum wind speed (W_{max}), wind speed (W_s), wind direction (W_d), wind speed range (W_{range}), average temperature (T_{avg}), clearness index (C) and Downward Thermal Infrared radiative flux (IR). These parameters, which represent the spectrum of commonly encountered meteorological parameters were selected based on previous studies which evaluated the relationships between different meteorological parameters and solar PV performance [23–25,27,32]. The 14 variables were selected and numerically analyzed using the Boruta algorithm in Python v3.8 to fully explore their influence on cell temperature. Having performed parameter correlation using the Boruta algorithm and analysed the importance of each and every parameter on cell temperature, a few prominent parameters were selected for simulation and model development. The 14 parameters were initially selected to ensure that as many parameters were analysed and no important parameter is missed in the analysis and modelling process.

In the analysis of these parameters, average temperature was taken as the response variable and the other parameters were used as the predictor variables. The selected parameters were used in developing the prediction model in Artificial Neural Networks (ANNs).

Artificial Neural Networks (ANNs) model

An Artificial Neural Network model was developed to establish the association between meteorological parameters against the ambient temperature which can be used to predict the temperature of PV collectors. Literature reveals that ANNs have been successfully used in situations where there is difficulty in establishing the relationship between the predictor and predicted variables both analytically and mathematically [4].

In this study, a feed forward backpropagation neural network was trained using the Levenberg-Marquardt algorithm. This training algorithm was selected due to its high computational speed notwithstanding that it also demands huge memory resources. The gradient descent learning algorithm with momentum was selected with input variables taken from the all-important variables obtained from the Boruta algorithm. All the values used in this study were normalised in the range 0 - 1 as shown by Eq. (1). Original non-normalised values were obtained by employing Eq. (2).

$$V_n = \frac{V - V_{\min}}{V_{\max} - V_{\min}} \tag{1}$$

$$V_p = V_n(V_{\max} - V_{\min}) + V_{\min} \tag{2}$$

Where: V_n is the normalised value, V_{min} is the minimum measured value, V_{max} is the measured maximum value while V_p is the value predicted by the ANN model.

All the relevant features obtained from Boruta algorithm were used as input parameters. The ANN had a single hidden layer having neurons which were varied between 10 and 50 with a step of five. The ANN also had a single output layer with temperature as the target value. Selection of the best performing combination of activation functions for both the hidden and output layer was done. All the different combinations of two of the three assessed activation functions were analysed for their performance in an ANN with a fixed number neurons equal to 25. The transfer functions evaluated were pure linear (purelin), hyperbolic tangent sigmoid (tansig) and logistic sigmoid (losig).

One combination of transfer functions was used to select the best number of neurons to be used in the modelling process. There was random initialisation of the weights used in model development. A ratio of 70:15:15 was used to assign data, respectively, for training, testing and validation. 3652 data sets obtained from NASA for the period 2009 to 2019, was thus split for training, testing and validation with respective number of datasets given by 2556, 548 and 548. The ANN toolbox in in MATLAB® release R2018a was used in the modelling process.

To evaluate the validity of the ANN model, data not previously used in the training phase was used to evaluate the performance of the developed ANN model. Evaluation metrics such as the coefficient of determinationR^2, mean absolute percentage error (MAPE), and residual mean square error (RMSE) were used and these are given by Eqs. (3)–(5).

$$R^2_{adj} = 1 - \left(1 + \frac{\sum_{i=1}^{n}\left(y_i - \hat{y}_i\right)^2}{\sum_{i=1}^{n}(y_i - \bar{y}_i)^2}\right)\frac{(n-1)}{(n-p-1)} \tag{3}$$

$$MAPE = \left(\frac{1}{n}\sum_{i=1}^{n}\left|\frac{y_i - \hat{y}_i}{y_i}\right|\right) \times 100\% \tag{4}$$

$$RMSE = \sqrt{\left(\frac{1}{n}\sum_{i=1}^{n}\left|y_i - \hat{y}_i\right|^2\right)} \tag{5}$$

Where; y_i is the i^{th} observed value, $\bar{y}$ is the sample mean, $\hat{y}_i$ is the predicted i^{th} value, p is the number of independent variables and n is the sample size.

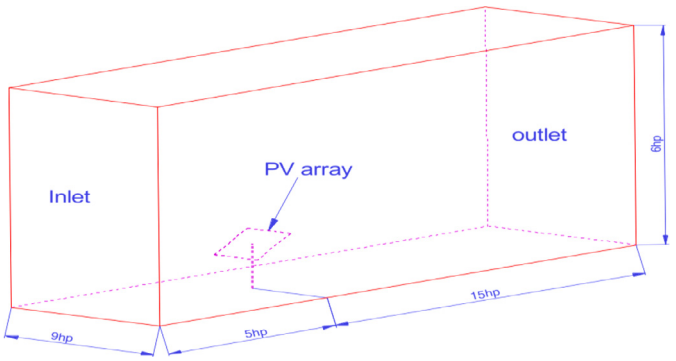

Fig. 2. Computational domain.

Experimental design

Different variations of the installation configurations to analyse their effect on array temperature were obtained using face centred, central composite design of experiments implemented using Design Expert software v12.0. The parameters used in the experimental design are tilt, orientation and, wind speed and direction. Tilt angles were varied from 8º to 38º and the installation orientation (azimuth) had values varying from -22.5º (North of North West, NNW) to 22.5º (North of North East, NNE).

The wind direction and speed assumed values obtained from NASA through the use of User Defined Functions (UDFs). The results obtained from the CFD simulations with varying installation parameters were used to generate a response surface for mapping the relationship between installation parameters, temperature and energy generated by a solar PV module.

Simulations using computational fluid dynamics (CFD)

The Reynolds Averaged Navier Stokes (RANS) governing Equations represented by Eq. (6) were used to model the air flow around the PV array. The turbulence model, SST k-ω shown by Eq. (7) and (8) was adopted to compute the turbulent behaviour of the flowing fluid air. One of the most widely used turbulence model, the SST k-ω turbulence model was chosen because of its wide applications in engineering flow problems. This is due to its stability, simplicity and its high accuracy in predicting mean flow profiles [13,19].

$$\rho\frac{\partial\bar{\emptyset}}{\partial t}+\rho\bar{u}_j\frac{\partial\bar{\emptyset}}{\partial x_j}-\frac{\partial}{\partial x_j}\left[\Gamma_{\emptyset,\mathrm{eff}}\frac{\partial\bar{\emptyset}}{\partial x_j}\right]=S_{\emptyset} \tag{6}$$

Where; $\rho(\mathrm{kg/m^3})$ is the density, while time taken is t (seconds) and the velocity vector is **u** (m/s). κ (W/mK) is the thermal conductivity and the independent flow variable is $\emptyset$. $\Gamma_{\emptyset,\mathrm{eff}}$ $(\mathrm{m^2/s})$ represents the effective diffusion coefficient while $S_{\emptyset}$ is the source term.

$$\frac{\partial}{\partial t}(\rho k)+\frac{\partial}{\partial x_i}(\rho k u_i)=\frac{\partial}{\partial x_j}\left(\xi_k\frac{\partial k}{\partial x_j}\right)+g_k-y_k+s_k \tag{7}$$

$$\frac{\partial}{\partial t}(\rho\omega)+\frac{\partial}{\partial x_i}(\rho\omega u_i)=\frac{\partial}{\partial x_j}\left(\xi_\omega\frac{\partial\omega}{\partial x_j}\right)+g_\omega-y_\omega+d_\omega+s_\omega \tag{8}$$

Where; g_k is the turbulent kinetic energy generation term; g_ω is the specific dissipation rate generation term; ξ_ω and ξ_k are, respectively, the effective diffusivity of ω and k. The dissipation rates of k and ω are, respectively, given by y_k and y_ω; The cross diffusion term is given by d_ω; The user defined source terms taken as zero in this study are represented by s_k and s_ω.

The geometry used in the simulation was developed using ANSYS design Modeller v17.0 and it mimicked the geometry used by Abiola-Ogedengbe [22] in his wind tunnel experiments. The ground mounted PV array had its tilt and orientation, respectively, varied from 8º to 38º and -22.5º to 22.5º while its height of installation h_p was 1.5m. The UDFs (file) were used to provide the values of wind speed and wind direction. Respective dimensions of 21.4 h_p, 6 h_p and 9 h_p were used for the length, height and width of the computational domain. $5h_p$ and $15h_p$ were, respectively, the distances from the inlet to the PV array and from the PV array to the outlet of the computational domain. These dimensions guaranteed no obstruction of air flow on the PV array surface as shown in Fig. 2.

A mesh of structured grids was developed using ANSYS ICEM 17. This mesh had 600 000 nodes and was adopted after a mesh independence study. Grid independence study was performed to determine the minimum grid size that gives the best results. Three grids namely coarse, medium and fine with number of elements given by 45 415, 175 728 and 600 313,

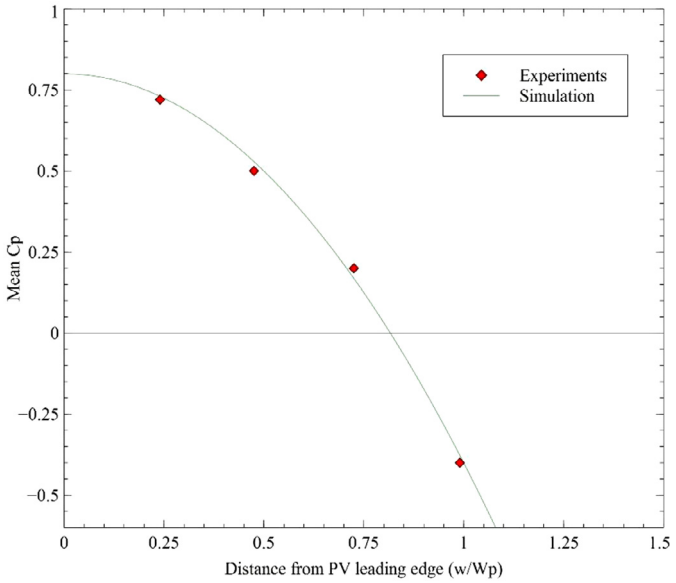

Fig. 3. Experimental validation of the mean pressure coefficient (Cp).

respectively, were evaluated and a grid size of 600 313 was found to be having better performance. To ascertain the best performing grid for the problem, further steps in grid refinement were taken at a rate of 20% additional nodes with each step and four more meshes were evaluated and these were 720 376, 864 451, 1 037 341 and 1 244 810 and the grid with the minimum number of elements that give accurate results was selected. In this case, a grid of 864 451 nodes was chosen.

The Finite Volume Method (FVM) was adopted in resolving wind flow conservation equations. Pressure and velocity flow fields were decoupled by employing the SIMPLE algorithm. Diffusion and convection terms were discretised by making use of the second-order upwind scheme represented by Eq. (9) [34].

$$\gamma_{f,sou} = \gamma + \gamma_{grad}.\vec{r} \tag{9}$$

Where; the face value using second order upwind is given by $\gamma_{f,sou}$; The cell-centred value γ had its gradient γ_{grad} in the cell upstream; The displacement vector $\vec{r}$ is measured from the face centroid to upstream cell centroid. Simulations were done to compute airflow fields on the PV module. The pressure coefficient, C_p profile obtained in the simulations was validated against the pressure coefficient profile obtained by Tominaga et al. [28]. The C_p from simulations had a percentage difference of 1.03% with the C_p from experimental studies and hence the simulation model was concluded to be able to precisely compute the airflow fields around the PV collector.

The boundary conditions for the Atmospheric Boundary Layer (ABL) to be used were as follows: Inlet into the computational domain was treated as velocity inlet with user-defined functions derived from measured data while the outlet was treated as a pressure outlet. All walls were given a No-slip wall condition. The discretisation scheme for momentum, TKE and dissipation rate was second order upwind. The Pressure-velocity coupling method used the SIMPLE algorithm.

CFD model validation

Air flow fields around the solar PV module were simulated to determine the temperature on the solar PV module and these were validated using experimental data by Abiola-Ogedengbe's [22] results of wind tunnel experiments as shown in Fig. 3. In Fig. 3, w represents the distance measured along the solar panel width from the leading edge and W_p is solar panel width. A 1.3% difference in the results obtained in the simulation model was found compared to the experimental results.

An HP Z6 G4 Workstation, Intel Xeon W-3223 8 Core 3.5Ghz equipped with 64GB RAM and an Nvidia Quadro RTX 4000 8GB Graphics card was used to run the simulations. The simulation was run for 36.8 h until the results were obtained.

Thermal Losses, temperature and radiation modelling

The solar ray tracing model was used for the selected location (Harare). Radiation flux was obtained from the Stefan-Boltzmann relationship given by Eq. (10) where the Stefan-Boltzmann constant,$\sigma = 5.67\text{x}10^{-8}$.$A_s$ is the surface area, ε is the emissivity (assumed to be 1), T_p is the temperature of the sun while T_s is the temperature of the surroundings.

$$q = A_s \varepsilon \sigma \left(T_p^4 - T_s^4\right) \tag{10}$$

The thermal losses incorporated in PVsyst were determined using the relationship shown by Eq. (11); Where, U is the thermal behaviour, T_c is the temperature of the solar cell, T_a is the ambient temperature, α is the absorption coefficient, H is the global horizontal irradiance while η is the PV cell efficiency.

$$U(T_c - T_a) = \alpha H(1 - \eta) \tag{11}$$

Optimisation

The CFD simulation results were used to determine the optimum configuration for minimising temperature while maximising energy generated. Response Surface Methodology (RSM) was employed to generate a 2nd order polynomial modelling the relationship between installation configurations, temperature and energy. The resulting temperatures from different simulations were used to simulate energy production using PVSyst for a full year. An empirical model (Eq. (12)) was used for predicting solar radiation availability on a tilted PV module surface. This radiation on a tilted PV module, I_t is obtained from the Global Horizontal Irradiance (GHI) which is obtained from Reflected Irradiance (I_r), Diffuse Irradiance and (I_d) Beam Irradiance (I_b), where; r_b, r_r and r_d are tilt factors for beam, reflected and diffuse irradiance.

$$I_t = I_b r_b + I_d r_d + (I_b + I_d) r_r \tag{12}$$

Results and discussions

Solar radiation and energy generated

The collectors were facing the general north direction i.e. North of North West (NNW), North (N) and North of North East (NNE) to harvest as much energy as possible. The different combinations of tilt (from 5° to 44°) and orientation (from -22.5° to 22.5°) were assessed. The simulations revealed that the maximum possible annual energy loss obtained after varying the parameters within the specified range was 5.1% as shown in Table 1 and Table SM1. However, the range between 8° and 38° was chosen for optimisation in this study and the maximum energy loss within this range was found to be 2.5% which is reasonably low. This range was chosen based on the generally accepted deviation in tilt angle of $\phi \pm 15°$ where ϕ is the latitude of the location [11].

The variation of energy generated with the tilt angle was modelled using a quadratic function as shown by Eqs. (13)–(15), respectively, for 0°, -22.5° and 22.5° azimuth angles where y is the energy generated and x is the tilt angle.

$$y = 1897.28 + 11.18x - 0.24x^2 \tag{13}$$

$$y = 1897.82 + 10.30x - 0.23x^2 \tag{14}$$

$$y = 1897.60 + 10.22x - 0.23x^2 \tag{15}$$

It was found that when the orientation is facing due west, there is slightly more energy generated compared to orientations due east. It is also revealed that the variation of energy generated with respect to tilt angle can be modelled using a quadratic polynomial.

Parameter correlation analysis and selection of controllable parameters

Parameter correlation was performed in random forests applying the Boruta algorithm. The RandomizedSearchCV obtained from sklearn was used to optimise the hyper parameters. Four variables were selected by the algorithm and these were pressure, humidity, wind speed, and wind direction. These parameters were selected with a test accuracy of 96.4%. The parameter selection indicate that wind direction, wind speed, humidity and pressure are closely correlated to ambient temperature. However, of these parameters, two are controllable and the other two are not controllable. Wind speed and direction are controllable parameters on installation configuration while pressure and humidity are non-controllable and hence cannot be used for temperature mitigation. However, these parameters are essential in predictive modelling of ambient temperature (See Fig. SM1).

The correlation matrix used for variable selection shows that pressure has a very strong correlation with temperature. Other factors of influence include precipitation and clearness index as shown in Fig. SM2. The relationship between pressure, relative humidity, wind speed and, wind direction was analysed and the graphs are shown in Fig. SM3.

The correlation of each of the selected variables with temperature was analysed using regression analysis. As shown in Fig. SM3, the coefficients of determination R^2 values of relative humidity, pressure, wind direction and wind speed are, respectively, 50.92%, 17.24%, 12.04% and 25.21%. The individual correlations show that relative humidity has the strongest correlation with temperature followed by wind speed.

From the parameter correlation analysis, some controllable parameters were selected. It was shown that the maximum and average wind speeds are, respectively, 9.22 and 3.56 m/s. (See Fig. SM4). The general wind direction is from the East

Table 1
Energy generated and losses for each configuration.

	Factor		Response	
Run	**B:Orientation (°)**	**A:Tilt (°)**	**Annual energy (kWh/m^2)**	**Energy loss (%)**
1	0	5	1947	2.90
2	0	8	1971	1.70
3	0	11	1991	0.70
4	0	14	2007	0.00
5	0	17	2018	0.00
6	0	20	2024	0.00
7	0	23	2026	0.00
8	0	26	2024	0.00
9	0	29	2017	0.00
10	0	32	2006	0.00
11	0	35	1991	0.70
12	0	38	1972	1.70
13	0	41	1948	2.90
14	0	44	1920	4.30
15	-22.5	5	1944	3.10
16	-22.5	8	1966	1.90
17	-22.5	11	1984	1.00
18	-22.5	14	1997	0.40
19	-22.5	17	2007	0.00
20	-22.5	20	2013	0.00
21	-22.5	23	2014	0.00
22	-22.5	26	2011	0.00
23	-22.5	29	2004	0.00
24	-22.5	32	1993	0.60
25	-22.5	35	1978	1.30
26	-22.5	38	1959	2.30
27	-22.5	41	1937	3.40
28	-22.5	44	1909	4.80
29	22.5	5	1943	3.10
30	22.5	8	1965	2.00
31	22.5	11	1983	1.10
32	22.5	14	1996	0.50
33	22.5	17	2005	0.00
34	22.5	20	2011	0.00
35	22.5	23	2012	0.00
36	22.5	26	2008	0.00
37	22.5	29	2001	0.20
38	22.5	32	1990	0.80
39	22.5	35	1975	1.50
40	22.5	38	1955	2.50
41	22.5	41	1934	3.70
42	22.5	44	1893	5.10

especially from ENE to NNE. Such a phenomenon will make the collector facing NNE have more direct interactions with the wind while the NNW configuration has less direct interactions with the wind thereby experiencing less temperature reduction.

Temperature prediction model

An ANN prediction model was developed and run in Matlab 2018a. The assessment of activation functions revealed that the Logistic Sigmoid transfer function in the hidden layer and the pure linear activation function in the output layer performed the best for all combinations of activation functions evaluated in this study (See Table SM2). A total of 35 neurons were selected and used in the model as they gave the best results and this is outlined in Table SM3.

The ANN model was developed in Matlab and was found to perform well with R^2 values above 90%. Fig. SM5 reveals the performance validation of the developed ANN model. The predicted values of ambient temperature were compared to the expected values and the model was found to have a coefficient of determination of 90.85%.

CFD simulation results

Profiles of air flow velocity

The wind flow characteristics around the PV module were used to deduce the rate of heating of solar PV modules with varying installation configurations (Fig. SM6). The results show some complex airflow velocity fields around the solar col-

lector and this results from the presence of the solar PV array as a wind barrier thus hindering free flow of wind. This occurrence was also reported in a study by Lu and Zhao [18].

The velocity fields are different for different tilt angles with less obstructions occurring at lower tilt angles and higher obstructions being recorded on steeper tilt angles. Steeper tilt angles resulted in more wind-PV interactions thus causing more cooling in steeper tilt angles compared to less steep tilt angles. This was as a result of a larger effective surface area exposed to the flowing wind by steeper tilt angles. Lower impact wind velocities were recorded on lower tilt angles compared to the steeper tilt angles. An average of 9.99 m/s impact velocity was experienced on the 8º tilt angle configuration against an average impact velocity of 10.03 m/s for steeper tilt angles. This is the reason for more cooling occurring on higher tilt angles while less cooling occurs on lower tilt angles. Both average temperatures (T_{avg}) and maximum temperatures (T_{max}) were found to be increasingly lower with increasing tilt angle.

TKE profiles

The results indicate that higher tilt angles cause higher turbulences and hence TKE values increased with increasing tilt angles. As shown in Fig. SM7, the results gave average TKE values of 0.264 m^2/s^2, 0.316 m^2/s^2 and 0.395 $m^2/s^{2,}$ respectively, for 8º, 23º, and 38º. Higher turbulences experienced on higher tilt angles are the reason for the lower temperatures experienced on steeper tilt angles compared to lower tilt angles. This is because higher wind turbulences have a tendency of dissipating the heat generated on the PV collector.

The orientation of installation also shows its importance in the cooling of the solar PV arrays as evident from the 22.5º (Figure SM8) configuration which shows higher turbulences compared to other configurations. This is expected since more wind flow was expected in that direction compared to other directions.

Temperature profiles

The simulations in this study used JA Solar PV module. In this case T_{NOCT} was taken as 45 °C. The results were validated against the established relationship (Eq. 16) to calculate the cell temperature given the ambient temperature. There was only a 0.28 % average prediction error in the CFD model when compared to the results obtained from Eq. 16. The results obtained in the CFD simulations indicate a 5 % increase in average temperature for 8º tilt and a 3 % average decrease in temperature for 38º tilt angle when both are compared to the 23º tilt angle.

$$T_c = T_a + (T_{NOCT} - 20)\frac{G}{800} \tag{16}$$

From Fig. 4, the PV module temperature profiles are shown and the profiles indicate that more heating was experienced on the 8º tilt followed by 23º and then 38º tilt angles. The profiles reveal that the temperatures experienced on the solar PV module are well above the ambient temperatures for all configurations. These high temperatures result in energy losses.

Velocity streamlines

Air flow velocity streamlines around the solar PV collector are shown in Fig. SM9. These streamlines characterise the path followed by fluid air particles and they describe flow in terms of velocity and direction. The flow velocity and the spacing between the streamlines are inversely proportional to each other.

There are turbulent eddies behind the PV module for all configurations. These turbulent eddies were much closer to the PV module for the 38º tilt and this had an effect of causing more cooling compared to the other tilt angles.

Response surface modelling

The values of average solar PV module temperature, maximum PV module temperature reached, TKE and average velocity were obtained from the simulations. Response Surface Methodology (RSM) was used to analyse these results and models were developed from these results.

Temperature as the most important output variable was analysed against the installation variables used in this study. The results revealed that the tilt angle and the orientation had a strong relationship with PV module temperature. The simulation results were used to generate contours and response surfaces shown in Fig. 5 and the analysis of the contours generated was performed. The analysis of both the contours and the response surface revealed that both the tilt and the azimuth angle of installation had a significant contribution to the PV module temperature. It is evident that at the minimum azimuth of -22.5º and a tilt of 8º there is maximum temperature generation. This is validated by the fact that the wind direction in this study was found to be mainly concentrated on the eastern direction and hence more cooling was expected in the eastern orientation compared to the western orientation. The minimum temperatures were attained at an orientation of 22.5º and tilt of 38º with temperatures in the range of 30º. Also a tilt of 8º at an orientation of 22.5º gave a temperatures around 50 °C experienced in this simulation. Tilt angles from 20º to 38º at orientations between 0º and 22.5º gave cell temperatures of 40 °C and below.

Numerical optimization and economic analysis

Minimising temperature

Numerical optimisation was performed in Design Expert v.12.0 to determine the configuration that gives the minimum possible temperature rise on the solar PV array as shown by Fig. SM10. The input parameters used were the tilt angle and

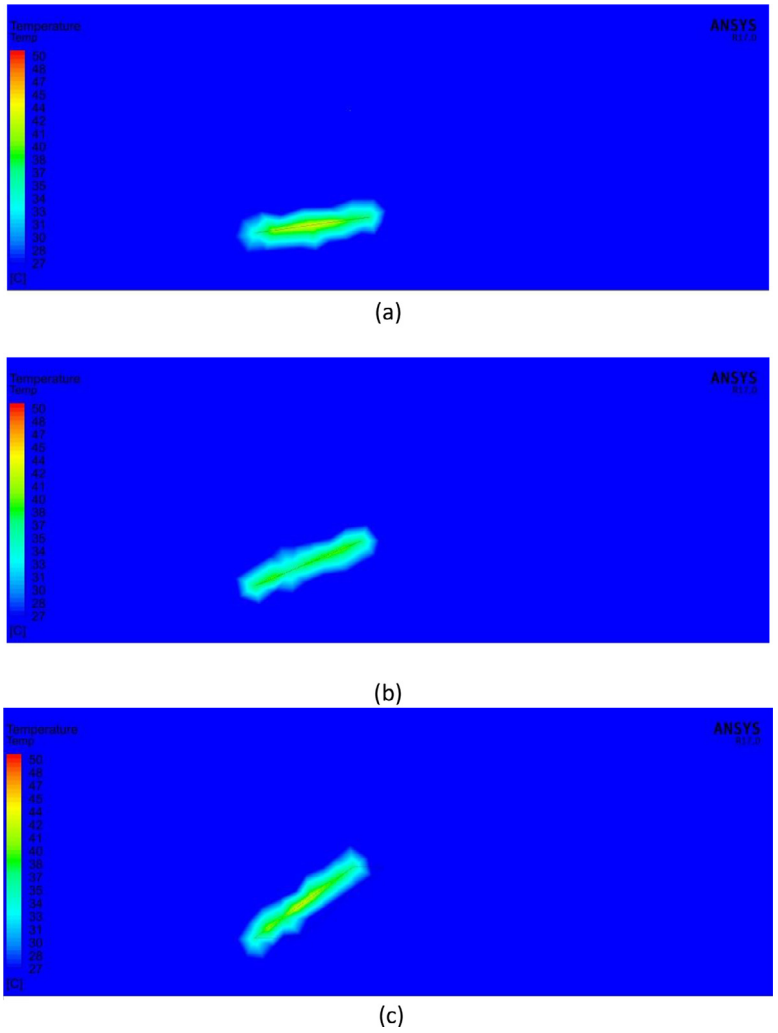

Fig. 4. Temperature profiles at 0º orientation; (a) 8º tilt, (b) 23º tilt (c) 38º tilt.

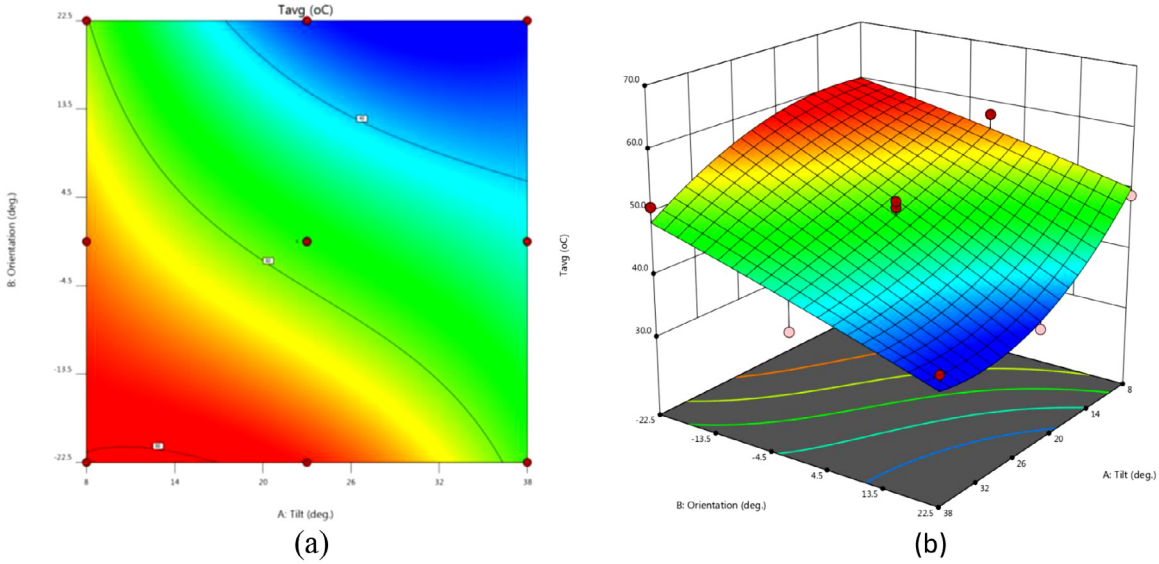

Fig. 5. Average temperature contours Response surface for the average temperature.

the orientation while the output parameter was the temperature rise. The optimisation revealed a tilt of 35.42 º and an orientation of 22.15º. This configuration gave an average temperature of 34.1 °C and a maximum temperature of 50.38 °C. On the other hand, the average velocity experienced was 10.06 m/s while the TKE associated with such a configuration was 0.35 m^2/s^2. The optimisation shows that for tilt angles above 20º and orientations above 5º, there is low temperature generated and hence the optimum solution lies in this region.

Optimization for energy generation

The results from the simulation studies were used to run simulations in PVsyst to determine the annual energy generated on a hypothetical 25 kW solar PV array under different temperatures as obtained from CFD simulations as shown by Fig. SM11 and SM12. Different values of the thermal parameter (U) were obtained from CFD simulations and used in the PVsyst energy simulations. The 25 kW PV array was chosen based on the limitations of the free software version PVSyst 6.7 available. The values of ambient temperature and global irradiance were taken as the daily average and each day had its own values. The efficiency of the PV cells was taken as 18.9 % while the absorptivity was taken as 0.9.

The simulations in PVsyst were used to select an optimum configuration for maximising the energy generated. The Installation configuration was optimised using the tilt, orientation and the cell temperature as the input parameters. The annual energy generated under these different parameters was taken as the output. RSM was used to optimise the configuration to select the one with the highest energy output. A quadratic polynomial was selected for the response surface generation. It is revealed that tilt angle values from 23º up to 35° combined with an orientation between 5º and 22.5º have a positive influence on energy generated. Tilt angles greater than 35º proved to be detrimental to power generation evident from the low power output. The results reveal that, as the orientation change from 5º (N) to 22.5º (NNE) there is a significant improvement in energy generated.

The optimisation of the installation configuration gives a tilt of 28.2º, orientation of 13.2º which results in 39.9 MWh of energy generated.

Energy gained due to temperature minimisation

A comparison of the energy generated with and without optimisation was performed. The comparison revealed that installation optimisation using Response Surface Optimisation results in extra 1.5MWh of energy being generated and this is equivalent to 3.9 % more energy generated. Considering a Feed-in-Tariff of US$0.15, this translates to an additional annual income of US$225 which is a revenue of US$5625 in the expected lifetime of the 25 kW solar PV plant of 25 years

The economic gain obtained from the different optimisation techniques is outlined in Table SM4 where 'General' implies the generally accepted optimum configuration of 0ºN and 23º tilt angle. It is shown that there is more power generated by temperature optimised configuration when compared to the general configuration. There are higher values of NPV, IRR and lower values of payback for the temperature optimised configuration.

Conclusions and recommendations

The study investigated the factors contributing to the temperature characteristics of a solar photovoltaic cell. Up to 14 meteorological parameters were evaluated and out of these 4 were selected for the development of a predictive model using Artificial Neural Networks. The model developed was found to be accurate with a coefficient of determination (R^2) of 93.1 %. The temperature distribution experienced on the PV collectors was also investigated. The turbulent air flow characteristic behaviour on a hypothetical 25 kW solar system was analyzed using a three dimensional computational fluid dynamics model. The impact of the installation azimuth and tilt as well as that of the meteorological parameters on temperature characteristics was analyzed. A Response Surface Methodology based optimization model was developed and, in this study several observations were noted as follows:

- Temperature can be accurately predicted using pressure, humidity, wind speed and direction with a coefficient of determination (R^2) of 93.1 %.
- The air flow velocity fields and the temperature characteristics are dependent on the installation configuration and the meteorological parameters such as wind direction and speed.
- Steep tilt angles experience higher impact wind velocities unlike less steep installation angles. Low tilt angles experience a broader spectrum of impact velocities, henceforth higher temperatures were recorded.
- Optimisation of the installation tilt was found to significantly reduce the temperature rise on the solar photovoltaic array while maximizing the energy generated by the solar photovoltaic array. The optimization performed was able to increase the energy generated by 3.9 %, thus increasing the total lifetime energy harvested by US$5625.
- The generally agreed tilt and orientation of 23º and 0º North are not always the best configuration for solar photovoltaic installations in Zimbabwe. A configuration of 28.2º tilt and 13.2º azimuth gave the optimum energy generated with an average annual cell temperature of 29.3 °C. This resulted in 3.9 % extra energy being generated.

Declaration of Competing Interest

The authors declare that they have no known competing financial interests or personal relationships that could have appeared to influence the work reported in this paper. This research received no specific grant from any funding agency in the public, commercial, or not-for-profit sectors.

Supplementary materials

Supplementary material associated with this article can be found, in the online version, at doi:10.1016/j.sciaf.2022.e01266.

References

[1] A. Ahadi, H. Hayati, J. Mitra, et al., A new method for estimating the longevity and degradation of photovoltaic systems considering weather states, Front. Energy 10 (2016) 277–285, doi:10.1007/s11708-016-0400-3.
[2] M.A. Al-Nimr, S. Kiwan, H. Sharadga, Simulation of a novel hybrid solar photovoltaic/wind system to maintain the cell surface temperature and to generate electricity, Int. J. Energy Res. 42 (2018) 985–998, doi:10.1002/er.3885.
[3] K. Chiteka, R. Arora, V. Jain, CFD Prediction of dust deposition and installation parametric optimisation for soiling mitigation in non-tracking solar PV modules, Int. J. Ambient Energy 42 (2021) 1307–1320, doi:10.1080/01430750.2019.1594373.
[4] R. Conceição, H.G. Silva, M. Collares-Pereira, CSP mirror soiling characterization and modeling, Sol. Energy Mater. Sol. Cells 185 (2018) 233–239, doi:10.1016/j.solmat.2018.05.035.
[5] S. Dubey, J.N. Sarvaiya, B. Seshadri, Temperature dependent photovoltaic (PV) efficiency and its effect on PV production in the world – a review, Energy Proced. 33 (2013) 311–321, doi:10.1016/j.egypro.2013.05.072.
[6] A.K. Goel, S.N. Singh, Thermal performance of solar air heater using jet impingement technique with longitudinal fins, JSIR 76 (2017) 12 December 2017.
[7] A.K. Goel, S.N. Singh, Performance studies of a jet plate solar air heater with longitudinal fins, Int. J. Ambient Energy 40 (2019) 119–127, doi:10.1080/01430750.2017.1372808.
[8] A.K. Goel, S.N. Singh, Influence of fin density on the performance of an impinging jet with fins type solar air heater, Theory Pract. Sustain. Dev. 22 (2019) 5873–5886.
[9] A.K. Goel, S.N. Singh, Experimental study of heat transfer characteristics of an impinging jet solar air heater with fins, Environ. Dev. Sustain. 22 (2020) 3641–3653, doi:10.1007/s10668-019-00360-1.
[10] D. Goossens, R. Lundholm, H. Goverde, J. Govaerts, Effect of soiling on wind-induced cooling of photovoltaic modules and consequences for electrical performance, Sustain. Energy Technol. Assess. 34 (2019) 116–125, doi:10.1016/j.seta.2019.05.007.
[11] M. Hartner, A. Ortner, A. Hiesl, R. Haas, East to west – The optimal tilt angle and orientation of photovoltaic panels from an electricity system perspective, Appl. Energy 160 (2015) 94–107, doi:10.1016/j.apenergy.2015.08.097.
[12] J.K. Kaldellis, M. Kapsali, K.A. Kavadias, Temperature and wind speed impact on the efficiency of PV installations. Experience obtained from outdoor measurements in Greece, Renew. Energy 66 (2014) 612–624, doi:10.1016/j.renene.2013.12.041.
[13] S. Kohlstädt, M. Vynnycky, A. Neubauer, A. Gebauer-Teichmann, Comparative RANS turbulence modelling of lost salt core viability in high pressure die casting, Prog. Comput. Fluid Dyn. 19 (2019) 316–327, doi:10.1504/PCFD.2019.102054.
[14] K.A. Kumar, K. Sundareswaran, P.R. Venkateswaran, Performance study on a grid connected 20kWp solar photovoltaic installation in an industry in Tiruchirappalli (India), Energy Sustain. Dev. 23 (2014) 294–304, doi:10.1016/j.esd.2014.10.002.
[15] N.M. Kumar, S.K. Yadav, S.S. Chopra, et al., Operational performance of on-grid solar photovoltaic system integrated into pre-fabricated portable cabin buildings in warm and temperate climates, Energy Sustain. Dev. 57 (2020) 109–118, doi:10.1016/j.esd.2020.05.008.
[16] R. Kumar, M.A. Rosen, A critical review of photovoltaic–thermal solar collectors for air heating, Appl. Energy 88 (2011) 3603–3614, doi:10.1016/j.apenergy.2011.04.044.
[17] K.Y. Lau, C.W. Tan, A.H.M. Yatim, Effects of ambient temperatures, tilt angles, and orientations on hybrid photovoltaic/diesel systems under equatorial climates, Renew. Sustain. Energy Rev. 81 (2018) 2625–2636, doi:10.1016/j.rser.2017.06.068.
[18] H. Lu, W. Zhao, CFD prediction of dust pollution and impact on an isolated ground-mounted solar photovoltaic system, Renew. Energy 131 (2019) 829–840, doi:10.1016/j.renene.2018.07.112.
[19] F.R. Menter, Two-equation eddy-viscosity turbulence models for engineering applications, AIAA J. 32 (1994) 1598–1605, doi:10.2514/3.12149.
[20] P.A. Mirzaei, J. Carmeliet, Influence of the underneath cavity on buoyant-forced cooling of the integrated photovoltaic panels in building roof: a thermography study, Prog. Photovolt. Res. Appl. 23 (2015) 19–29, doi:10.1002/pip.2390.
[21] P.A. Mirzaei, E. Paterna, J. Carmeliet, Investigation of the role of cavity airflow on the performance of building-integrated photovoltaic panels, Sol. Energy 107 (2014) 510–522, doi:10.1016/j.solener.2014.05.003.
[22] A. Abiola-Ogedengbe, "Experimental investigation of wind effect on solar panels," The University of Western Ontario, 2013. Accessed: Jul. 04, 2022.
[23] I. Pujotomo, R. Aita Diantari, Characteristics surface temperature of solar cell polycrystalline type to output power, in: Proceedings of the E3S Conference 73:01008, 2018, doi:10.1051/e3sconf/20187301008.
[24] A. Razak, Y.M. Irwan, W.Z. Leow, et al., Investigation of the effect temperature on photovoltaic (PV) panel output performance, Int. J. Adv. Sci. Eng. Inform. Technol. 6 (2016) 682, doi:10.18517/ijaseit.6.5.938.
[25] S. Saglan, B. Oral, S. Gorgulu, Measurements of meteorological parameter effects on photovoltaic energy production, Int. J. Circ. Syst. Signal Process. 9 (2015) 240–246.
[26] J. Siecker, K. Kusakana, B.P. Numbi, A review of solar photovoltaic systems cooling technologies, Renew. Sustain. Energy Rev. 79 (2017) 192–203, doi:10.1016/j.rser.2017.05.053.
[27] N. Smith, A Study Of The Sensitivity Of Solar Power Generation To Varying Weather Conditions, University of North Dakota, 2018.
[28] Y. Tominaga, A.S. ichi, T. Kitahara, Y. Arinami, Air flow around isolated gable-roof buildings with different roof pitches: wind tunnel experiments and CFD simulations, Build. Environ. 84 (2015) 204–213, doi:10.1016/j.buildenv.2014.11.012.
[29] S. Vafaei, A. Rezvani, M. Gandomkar, M. Izadbakhsh, Enhancement of grid-connected photovoltaic system using ANFIS-GA under different circumstances, Front. Energy 9 (2015) 322–334, doi:10.1007/s11708-015-0362-x.
[30] I. Wole-Osho, H. Adun, M. Adedeji, et al., Effect of hybrid nanofluids mixture ratio on the performance of a photovoltaic thermal collector, Int. J. Energy Res. (2020), doi:10.1002/er.5619.
[31] S.K. Yadav, U. Bajpai, Performance evaluation of a rooftop solar photovoltaic power plant in Northern India, Energy Sustain. Dev. 43 (2018) 130–138, doi:10.1016/j.esd.2018.01.006.
[32] R.L. Yang, G.M. Tiepolo, É.A. Tonolo, et al., Photovoltaic cell temperature estimation for a grid-connect photovoltaic systems in Curitiba, Braz. Arch. Biol. Technol. 62 (2019) e19190016, doi:10.1590/1678-4324-smart-2019190016.
[33] R. Zhang, P.A. Mirzaei, J. Carmeliet, Prediction of the surface temperature of building-integrated photovoltaics: Development of a high accuracy correlation using computational fluid dynamics, Sol. Energy 147 (2017) 151–163, doi:10.1016/j.solener.2017.03.023.
[34] "ANSYS Fluent Theory Guide," vol. 15317, Release 15, November 2013, pp. 724–746, 2013.